Mean Vertical Motions Seen by Radar Wind Profilers

G. D. NASTROM

St. Cloud State University, St. Cloud, Minnesota

T. E. VANZANDT

Aeronomy Laboratory, NOAA, Boulder, Colorado

(Manuscript received 26 July 1993, in final form 10 December 1993)

ABSTRACT

Radar wind profilers have been used to measure directly the vertical motion above the radar site. Mean values of vertical motions in the troposphere and lower stratosphere reported at sites in and near mountains are often several centimeters per second and have often been attributed to the effects of quasi-stationary lee waves. However, observations now available at sites in the plains, far from any mountains, also show mean values of several centimeters per second. For example, monthly mean values seen by the Flatland VHF radar near Champaign–Urbana, Illinois, range from about -3 to -7 cm s^{-1}, with largest magnitudes during the winter. The authors examine several of the hypotheses that have previously been advanced to explain these observations and find that each is inconsistent with the observations in some respect, except that quasi-horizontal flow along gently sloping isentropic surfaces leads to mean downward motion as large as 1–2 cm s^{-1}. In this paper the authors suggest that the effects of vertically propagating gravity waves can account for most of the mean downward motions measured with radars, and the measured mean vertical motions can aptly be termed "apparent" mean vertical motions. In gravity waves with downward phase propagation (upward energy propagation), the perturbations to the static stability and to the vertical velocity are negatively correlated. Since the radar reflectivity is proportional to the static stability, regions of the radar sampling volume with downward (or less strongly upward) vertical air motion due to gravity waves are weighted more heavily. A model incorporating this suggestion is first developed for a monochromatic gravity wave and is then expanded to a spectrum of gravity waves. This model predicts a correlation between the magnitude of the downward motion seen by the radar and the gravity wave energy density; the predicted relationship is verified by the observations from the Flatland radar. Statistical analysis of data from Flatland suggests that in the midtroposphere about 60% of the gravity wave energy is contained in waves with downward propagation of phase. The present model for w applies to the reflectivity from any refractive-index irregularities that can be treated as passive scalars, whether they are in the neutral atmospheric density, aerosol density, or plasma density and whether they arise from isotropic turbulence, anisotropic turbulence, Fresnel scattering, etc.

1. Introduction

The vertical velocity of the air is a key variable in meteorology. Wind-profiling radars offer the unique capability of directly measuring the vertical velocity of the air. This capability has been amply demonstrated by measurement of the relatively large vertical velocity in mesoscale circulation systems such as convective cells and gravity waves (Crochet et al. 1990). The vertical velocity in the troposphere and lower stratosphere, however, is expected to be small in large-scale systems and in long-period time averages. On the contrary, early results from VHF profilers located near rough terrain, such as at Poker Flat, Alaska, often gave long-term mean vertical motions of several centimeters per second in the troposphere (e.g., Nastrom and Gage 1984). Such results were dismissed, however, as unrepresentative of the large-scale flow because they were contaminated by the effects of terrain (as reviewed by Gage 1990; Ecklund et al. 1982; Nastrom et al. 1985). The Flatland VHF radar was constructed in very flat terrain near Champaign–Urbana, Illinois (40.5°N, 88.5°W), to enable the study of long-term vertical motions free from terrain effects (Green et al. 1988).

Instead of being very small, however, the long-term mean vertical velocity $\bar{w}$ at Flatland is downward throughout the troposphere with a value of several centimeters per second when averaged over periods ranging from hours to months, rather than nearly zero as expected. For example, Fig. 1 shows the profiles of monthly $\bar{w}$ from the first year of operation, March 1987–February 1988. The results clearly show that the motions are downward in the troposphere and are usually slightly positive in the lower stratosphere (climatological heights of the tropopause at 30° and 40°N are indicated on the figure). Similar patterns of descent

Corresponding author address: Dr. Gregory D. Nastrom, Department of Earth Sciences, St. Cloud State University, 720 Fourth Avenue South, St. Cloud, MN 56301-4498.

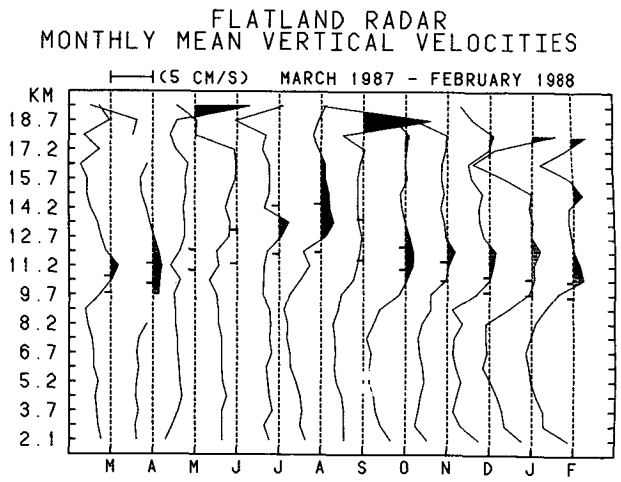

FIG. 1. Vertical profiles of the monthly mean vertical velocities at Flatland during March 1987–February 1988 measured with a vertically directed radar beam. Upward motions are shaded. Climatological heights of the tropopause at 30°N (upper) and 40°N (lower) are indicated by marks along the ordinate each month.

in the troposphere and ascent in the lower stratosphere are sometimes seen by radars at other sites (e.g., Fukao et al. 1991; Gage et al. 1991; Nastrom et al. 1993). Some of these occurrences have been attributed to special weather conditions, such as proximity to the jet stream at the MU radar or to convection in the National Oceanic and Atmospheric Administration (NOAA) equatorial chain of radars, and thus can be attributed to indirect circulation cells of ageostrophic origin or to radiative-cooling effects. The pattern seen at Flatland and Liberal, Kansas, however, has not yet been explained. Since $\bar{w}$ may represent processes in addition to air motion, it should properly be called "apparent" mean vertical motion, although we will refer to it as mean vertical motion in this paper. The purpose of this paper is to review some of the suggested causes for the Flatland observations of $\bar{w}$, such as flow along sloping isentropic surfaces, broadscale subsidence around small intense updrafts, and the effects of vertically propagating gravity waves, and to present the analyses that have been made to test these suggestions. Observations from the VHF radars at Flatland and at Liberal will be used here.

A brief history of the observations of mean vertical velocity at Flatland is given in section 2, along with a discussion of some of the proposed mechanisms that have been considered. Each of the mechanisms proposed in the past is found to be inconsistent with the Flatland and Liberal observations. Section 3 contains a discussion of the effects of vertically propagating gravity waves on apparent mean vertical motion and presents a model for the effect of gravity waves on the measured $\bar{w}$. Predictions from this model of gravity wave effects are compared with observations in section 4. Sections 5 and 6 contain a brief discussion, our conclusions, and a summary.

2. Observations of the mean vertical velocity

The Flatland radar has undergone numerous upgrades since 1987, evolving from a single vertical beam during the period shown in Fig. 1 to a full six-beam configuration at present (Warnock et al. 1993; Clark et al. 1993). Tests of some of the suggested explanations for $\bar{w} \neq 0$ have become possible only as the radar capability has matured. For example, Nastrom et al. (1990b) used data from a three-beam configuration of the radar to study flow along isentropic surfaces. One hypothesis is as follows: if the atmospheric flow is along isentropic surfaces to a first approximation and if the isentropic surfaces are inclined to the horizontal in the mean, then the vertical radar beam may detect the vertical component of motion along the isentropes. Indeed, this concept is central to the so-called adiabatic method used to infer vertical motions from radiosonde data and is discussed in standard textbooks such as Holton (1979). By correlating the horizontal winds seen by the radar with the slope of isentropic surfaces determined using the triangle of radiosonde stations encompassing Flatland, it was found that flow along tilted isentropes in the midtroposphere (near 5.6 km) could account for $\bar{w} \approx -1.5$ cm s^{-1} during February–March 1990. While -1.5 cm s^{-1} is relatively large, it is only a fraction of the -5.2 cm s^{-1} mean value measured during those months in Fig. 2. Of course, the horizontal spacing of the radiosonde sites, about 400 km, limits indirect estimates of $\bar{w}$ to relatively large-scale features. For long-term averages over the plains, however, this limitation is not expected to be a problem since other studies (e.g., Van den Dool 1990) have found smooth patterns in proxy indicators of vertical motion such as mean precipitation.

Another hypothesis involves convection: in regions of strong convection, it is expected that most upward mass transport occurs in intense updrafts, and that mass balance is maintained by gentle subsidence over a much larger area. Thermodynamic balance is maintained when the adiabatic warming due to subsidence offsets longwave radiational cooling of the air. Such motion systems are expected in the Tropics (e.g., Holton 1979; Balsley et al. 1988; Gage et al. 1991). At Flatland, if vertical motions in the small updraft areas were outside the dynamic range of the radar while the subsiding motions were within that range, the observations of vertical motion would be biased toward subsidence conditions and would show larger downward motion during cloudy conditions, when convection is enhanced. To test this suggestion, Nastrom et al. (1990b) compared mean vertical motions during times of clear or cloudy skies (as determined from surface observations at the Champaign–Urbana airport, located about 8 km east of Flatland). The monthly $\bar{w}$'s for the two

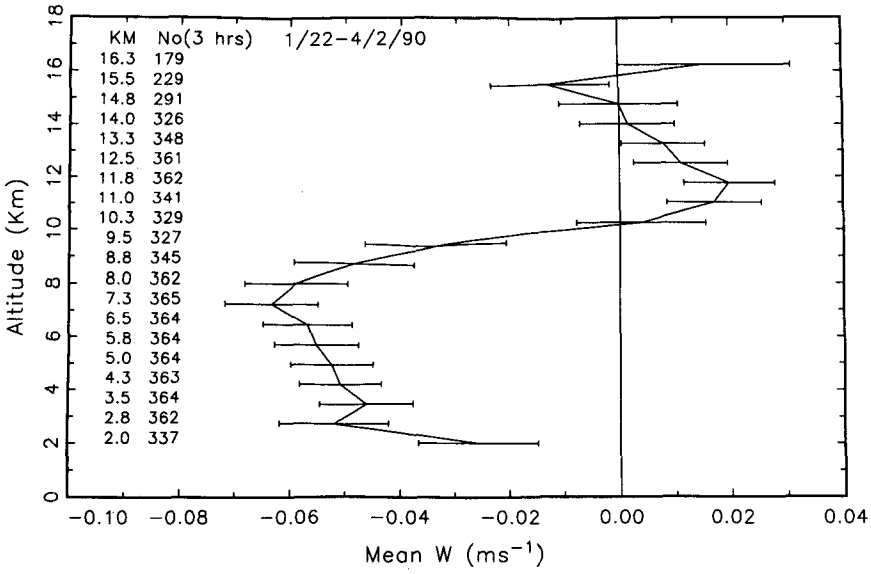

FIG. 2. Vertical profile of the mean vertical velocity at Flatland during 22 January–2 April 1990. The number of 3-h means averaged at each height is given; the error bars extend plus and minus one standard error of the mean.

sky conditions are nearly identical (Fig. 3), suggesting that the $\bar{w} \neq 0$ is not related to clouds. Further, the changes of $\bar{w}$ with season are small compared with the mean value (Fig. 1 and 4), as are the diurnal changes of hourly mean values seen at Liberal during early summer (Fig. 5). Since the intensity of convective activity changes both with season and with time of day in midlatitudes, these results indicate that $\bar{w} \neq 0$ is not explained by convection.

Several papers have noted that a small tilt of the nominally vertical beam could fold part of the horizontal velocity into the vertical beam, thus producing an apparent $\bar{w} \neq 0$ as reviewed by Gage (1990). But Clark et al. (1993) pointed out that at Flatland the observed $\bar{w}$ has not changed with time despite numerous system upgrades and beam-pointing checks. Figure 6 compares the annual $\bar{w}$ seen by the two electronically independent polarizations of the vertical antenna (curves N00 and E00) and $\bar{w}$ determined using opposing oblique beams in the north–south system (curve N15, S15). At most altitudes the (N15, S15) curve is not statistically very different from the other curves. There is a small, yet statistically significant, difference between the E00 and N00 curves; the reason for this difference is a topic of continuing study. Since the zonal and meridional wind profiles (not shown) are very different, it seems unlikely that simple beam tilting could account for the nonzero $\bar{w}$ (also, the mean zonal wind speed has a maximum near the tropopause, whereas $\bar{w}$ is zero there for all curves in Fig. 6). The close agreement of the estimate from oblique beams with those from the vertical beams in Fig. 6 also suggests that $\bar{w} \neq 0$ is not due to the tilted refractivity surfaces discussed by Palmer et al. (1991) because the oblique beams are tilted much further (15°) than any reflecting surfaces (Tsuda et al. 1988) and thus are free of aspect sensitivity. Further, McAfee et al. (1993) and Weber et al. (1992), with a shorter dataset, found high correlation between the $\bar{w}$'s seen by the 50- and 404-MHz radars at Platteville, Colorado; since there is no reported aspect sensitivity for UHF radars, this result also is inconsistent with effects from the tilted refractivity surfaces as hypothesized by Palmer et al. Finally, the biases of wind measurement due to horizontal shears as discussed by

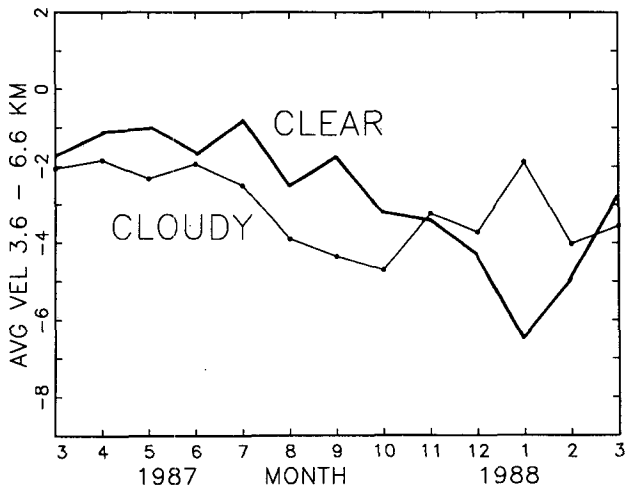

FIG. 3. Monthly mean vertical velocities at 3.6–6.6 km at Flatland sorted by sky condition at Champaign-Urbana airport (about 8 km east of Flatland). Partly cloudy conditions were not used.

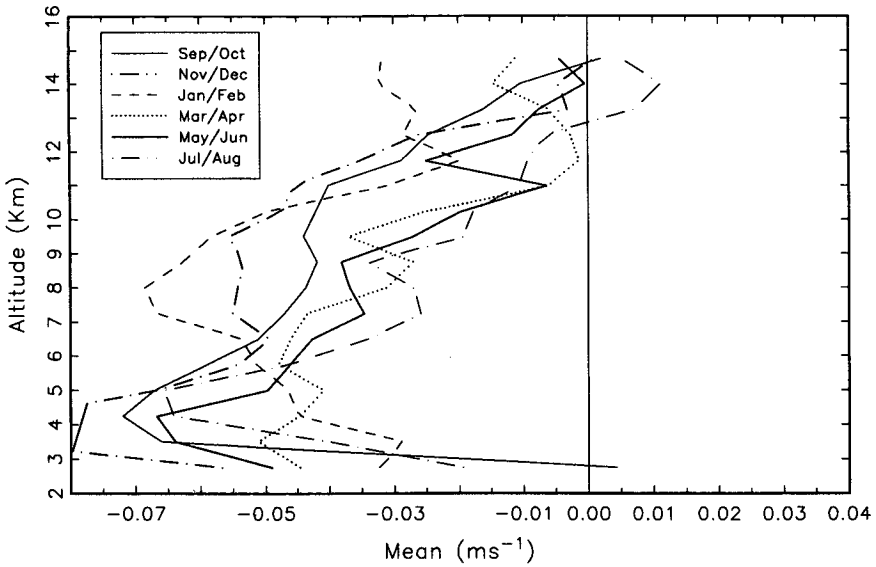

FIG. 4. Bimonthly means of vertical velocity at Flatland as seen by the vertical beam of the east–west antenna during September 1990–August 1991.

Kudeki et al. (1993) seem an unlikely mechanism for $\bar{w} \neq 0$ since they would grow with height rather than go to zero at the tropopause as observed.

In summary, we conclude that the observed vertical velocities at Flatland and Liberal are different from zero. The value of $\bar{w}$ is consistently near -4 cm s^{-1} in the troposphere during all hours of the day and during all seasons and approaches zero near the tropopause. The value of $\bar{w} \approx -4$ has persisted in all data taken since 1987. Each of the suggested causes considered so far has a shortcoming, although flow along sloping isentropes could account for a small portion of the mean vertical motion.

3. Gravity wave effects

The observed $\bar{w} \neq 0$ may be an artifact because of vertically propagating gravity waves. In a gravity wave with downward phase propagation, the perturbation vertical motion and the changes in static stability are in phase opposition. Since radar reflectivity is proportional to static stability, the apparent mean velocity in the sampling volume will then be weighted toward downward motions in a gravity wave with downward phase propagation. In this section we develop a model

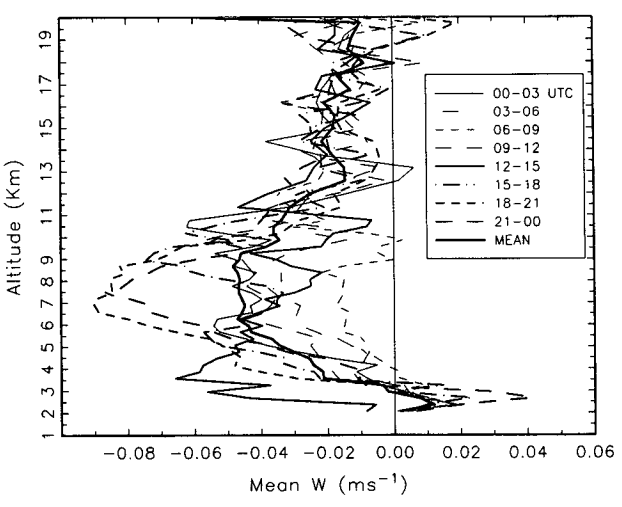

FIG. 5. Mean vertical velocities at Liberal, Kansas, measured with a vertically directed radar beam during May–June 1985, sorted according to time of day.

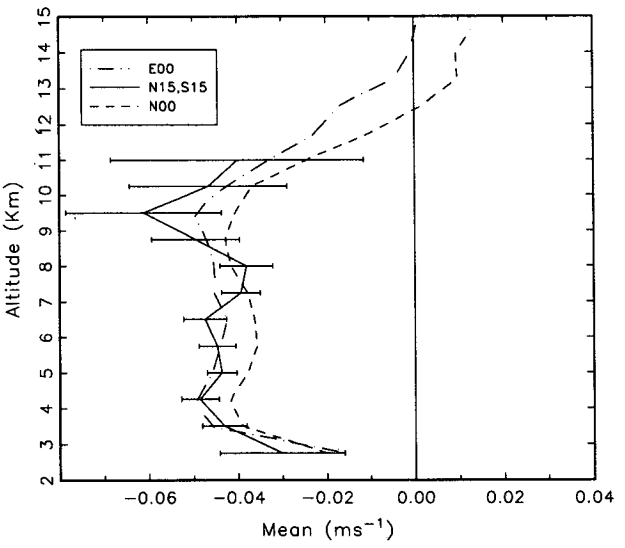

FIG. 6. Annual mean vertical velocities at Flatland during September 1990–August 1991 for the vertical beams on both antenna systems and as resolved by opposing oblique beams in the north–south plane.

for the apparent vertical velocity due to this mechanism. Among other things, this model predicts a relationship between the energy density of vertical velocity and $\bar{w}$. The predicted relationship is clearly found in the Flatland observations; therefore, we will go on to use the model and the observations to infer variables of the gravity wave field.

The radar reflectivity η depends on static stability. For isotropic, homogeneous turbulence it is [e.g., as reviewed by Gage (1990); our notation follows that of Gage (1990)]

$$\begin{aligned}\eta &= 0.38\lambda^{-1/3}C_n^2 \\ &= 0.38\lambda^{-1/3}(2.8L_0^{4/3}M^2) \\ &= 0.38\lambda^{-1/3}(2.8L_0^{4/3})\left(77\times10^{-6}\frac{P}{T\theta}\right)^2 \\ &\quad\times\left[\frac{\partial\theta}{\partial z}\left(1+\frac{15\,500q}{T}\right)-\frac{15\,500\theta}{2T}\frac{\partial q}{\partial z}\right]^2 \\ &= C_1\left[\frac{\partial\theta}{\partial z}\left(1+\frac{C_2q}{T}\right)-\frac{C_2\theta}{2T}\frac{\partial q}{\partial z}\right]^2, \end{aligned} \tag{1}$$

where C_n^2 is the refractivity turbulence structure constant and M^2 is the potential refractivity. The parameter C_1 is a function of the radar wavelength, λ; the turbulence intensity as parameterized by the outer scale of turbulence L_0, and the state of the atmosphere as given by P, T, θ; and the specific humidity q. For the moment we will assume that the variation of C_1 over the radar sampling volume is negligible compared to the quantity in square brackets and will proceed to develop a means to represent the vertical derivatives of θ and of q.

Gage (1990) reviews other mechanisms in addition to scatter from isotropic turbulence, principally scatter from anisotropic turbulence and Fresnel scattering from multiple stable layers. In the models reviewed for each scattering mechanism, the reflectivity, or backscattered power, is proportional to M^2. For anisotropic turbulence, $\eta_{\text{anisotropic}} = A_C\eta$, where A_C is a factor determined by the zenith angle of the beam and by the ratio of the correlation distances of the echoing region. For Fresnel scattering, the backscattered power P_r is proportional to F^2M^2, where F^2 is a function of the local spectrum of vertical displacements. The backscattered power P_r can be represented by an effective reflectivity $\eta_{\text{effective}}$ that could be used in Eq. (1). The point is that for each scattering mechanism, the form of the reflectivity equation is the same as Eq. (1), although the leading coefficient apparently changes. [In this context, it is noteworthy that Green et al. (1986), using vertical velocities measured with a vertically directed beam at the Sunset radar, found high correlation between velocities associated with quasi-specular reflection and those associated with turbulence scatter.] We will thus proceed to develop a theory using Eq. (1). Any given sample of radar observations, of course, may represent echoes due to a mixture of processes, in which case it is not clear what the leading coefficient should be. It will be shown below, however, that as long as the coefficient is constant over the sampling volume our theory does not depend on the coefficient.

The conservation of any passive scalar $S = \bar{S} + S'$ that has negligible horizontal gradients is given by

$$\frac{dS}{dt} = \frac{\partial S}{\partial t} + \mathbf{V}\cdot\nabla S \approx \frac{\partial S'}{\partial t} + w'\frac{d\bar{S}}{dz} \approx 0. \tag{2}$$

Assume that there are gravity waves of the form

$$\begin{aligned}&(w', S') \\ &= \text{Re}\{(\hat{w}, \hat{S})\exp[i(kx + ly + mz - \nu t + \phi)]\}, \end{aligned} \tag{3}$$

where k, l, m are the wavenumbers, ν is the frequency, and ϕ is the phase. Then, from Eq. (2),

$$\hat{S} = -\frac{i}{\nu}\frac{d\bar{S}}{dz}\hat{w}, \tag{4}$$

and it follows that

$$\frac{\partial S'}{\partial z} = \frac{m}{\nu}\frac{d\bar{S}}{dz}w'. \tag{5}$$

Then, Eqs. (4) and (5) lead to

$$\frac{dS}{dz} = \frac{d}{dz}(\bar{S} + S') = \frac{d\bar{S}}{dz}\left(1+\frac{m}{\nu}w'\right). \tag{6}$$

From Eqs. (1) and (6), taking θ and q for S, it follows that

$$\eta = C_1\left[\frac{d\bar{\theta}}{dz}\left(1+C_2\frac{q}{T}\right)-\frac{C_2\theta}{2T}\frac{d\bar{q}}{dz}\right]^2\left(1+\frac{m}{\nu}w'\right)^2. \tag{7}$$

Finally, if variations in L_0, P, T, q, and θ and changes in the vertical gradients of q and θ are relatively small over the sampling volume so that C_1 can be taken as constant for a given observation, Eq. (7) can be written as

$$\eta = \eta_0\left(1+\frac{m}{\nu}w'\right)^2. \tag{8}$$

Note that Eq. (5) with $S' = \theta'$ implies a negative correlation between w' and $\partial\theta'/\partial z$ when $\nu > 0$ and $m < 0$, which implies downward phase propagation and upward energy propagation, as would be expected with generation of gravity waves at low levels, such as in the planetary boundary layer. This negative correlation between w' and $\partial\theta'/\partial z$ leads to an apparent downward bias of vertical velocity in radar observations as shown by the theory to be developed next.

The observed vertical velocity over a sampling volume V and time interval T is

$$w_{\text{obs}} = \frac{\int_V \int_T \eta(\mathbf{r}, t, \phi) w'(\mathbf{r}, t, \phi) dt d\mathbf{r}}{\int_V \int_T \eta(\mathbf{r}, t, \phi) dt d\mathbf{r}}. \quad (9)$$

For the moment we will assume that the horizontal dimensions of the sampling volume are small relative to the horizontal scale of the gravity wave so that horizontal homogeneity can be assumed and integration over x and y is trivial. In general, this is probably a fairly good assumption; however, it turns out that even if it is not, the effect of averaging many observations to form a mean w obviates any dependence of mean w on the size of the sampling volume. Removing the dependence on x and y gives

$$w_{\text{obs}} = \frac{\int_0^Z \int_0^T \eta(z, t, \phi) w'(z, t, \phi) dt dz}{\int_0^Z \int_0^T \eta(z, t, \phi) dt dz}, \quad (10)$$

where Z is the vertical range resolution and T is the observation time interval.

Using Eq. (8), the integrand becomes

$$w_{\text{obs}} = \frac{\eta_0 \int_0^Z \int_0^T \left(w' + \frac{2m}{\nu} w'^2 + \frac{m^2}{\nu^2} w'^3 \right) dt dz}{\eta_0 \int_0^Z \int_0^T \left(1 + \frac{2m}{\nu} w' + \frac{m^2}{\nu^2} w'^2 \right) dt dz}. \quad (11)$$

The integration is performed using the form of w' given in Eq. (3) with the result

$$\begin{aligned} w_{\text{obs}} = \frac{1}{D} \Bigg\{ & \frac{\hat{w}}{\nu m} [\cos(mZ - \nu T + \phi) - \cos(-\nu T + \phi) - \cos(mZ + \phi) + \cos\phi] \\ & + \frac{\hat{w}^2}{4\nu^2} [\cos 2(mZ - \nu T + \phi) - \cos 2(-\nu T + \phi) - \cos 2(mZ + \phi) + \cos 2\phi] \\ & + ZT \frac{m\hat{w}^2}{\nu} + \frac{m\hat{w}^3}{36\nu^3} [\cos 3(mZ - \nu T + \phi) - \cos 3(-\nu T + \phi) - \cos 3(mZ + \phi) + \cos 3\phi] \\ & + \frac{3m\hat{w}^3}{4\nu^3} [\cos(mZ - \nu T + \phi) - \cos(-\nu T + \phi) - \cos(mZ + \phi) + \cos\phi] \Bigg\}, \end{aligned} \quad (12)$$

where

$$\begin{aligned} D = \Bigg\{ & ZT + \frac{2\hat{w}}{\nu^2} [\cos(mZ - \nu T + \phi) - \cos(-\nu T + \phi) - \cos(mZ + \phi) + \cos\phi] \\ & + \frac{m\hat{w}^2}{8\nu^3} [\cos 2(mZ - \nu T + \phi) - \cos 2(-\nu T + \phi) - \cos 2(mZ + \phi) + \cos 2\phi] + \frac{m^2\hat{w}^2}{2\nu^2} ZT \Bigg\}. \end{aligned}$$

Notice that if $Z = 2n\pi/m$ or $T = 2n\pi/\nu$, where n is an integer, only the third term of the numerator and the first and last terms of the denominator make nonzero contributions to w_{obs}, and $w_{\text{obs}} = m\hat{w}^2/\nu$, as shown by Nastrom et al. (1993).

In general, neither Z nor T is an integer number of cycles, and the value of any individual w_{obs} is a function of ϕ, as given by Eq. (12). However, averaging many observations together is equivalent to integrating over ϕ, since all phases are equally probable. Thus,

$$\bar{w} = \int_0^{2\pi} w_{\text{obs}}(\phi) d\phi = \frac{ZT(m/\nu)\hat{w}^2}{ZT[1 + 0.5(m\hat{w}/\nu)^2]}. \quad (13)$$

The last term in the denominator of Eq. (13) is negligible compared to the first term when the gravity wave is not near convective overturning. Under these conditions (Fritts 1984)

$$u' < |c - \bar{u}|. \quad (14)$$

Thus,

$$\left(\frac{u'}{c - \bar{u}} \right)^2 = \left(\frac{k}{\nu} u' \right)^2 = \left(\frac{\nu}{N} u' \frac{m}{\nu} \right)^2 = \left(\frac{m}{\nu} w' \right)^2 \ll 1. \quad (15)$$

At this level of approximation Eq. (13) yields

$$\bar{w} = \frac{m}{\nu} \hat{w}^2, \quad (16)$$

the same as for an integer number of cycles for Z or T. It is noteworthy that $\bar{w}$ is independent of the radar operating parameters T and Z in this model. Also, we note that if horizontal homogeneity had not been assumed in the integration of Eq. (9), then more terms would have appeared in Eq. (12), but they all would be removed by integration over ϕ.

When applied to a monochromatic wave with a typical vertical wavelength of 2000 m, period of 1500 s, and amplitude of 0.25 m s^{-1}, Eq. (16) gives $\bar{w} = -4.7$ cm s^{-1}. It is encouraging that this result is near the observed values of $\bar{w}$ reported by Nastrom et al. (1990b), Nastrom et al. (1993), and Clark et al. (1993).

Observed atmospheric vertical motions, however, represent a spectrum of gravity waves (VanZandt et al. 1991); thus, we here extend the analysis to a spectrum of waves. Following VanZandt and Fritts (1989) and VanZandt et al. (1991), we use a spectral model for $\hat{w}(m, \nu)$ that is variables separated. While the real spectrum cannot, of course, be truly variables separated [the conditions leading to Eq. (15) imply some coupling near wave saturation], this model should be an adequate approximation for the present estimations:

$$\hat{w}^2(\mu, \nu) = \left(\frac{\nu}{N}\right)^2 E_0 A(\mu) B(\nu), \quad f^2 \ll \nu^2. \quad (17)$$

Here, E_0 is the total (kinetic plus potential) energy, $\mu = m/m_*$, where m_* is the characteristic vertical wavenumber, and f is the inertial frequency. A modified form of the wavenumber spectrum of Desaubies (1976) is chosen: $A(\mu) = A_0\mu/(1 + \mu^4)$. Normalization as $\int_0^\infty A(\mu)d\mu = 1$ leads to $A_0 = 4/\pi$. The frequency spectrum $B = B_0\nu^{-p}$ is normalized as $\int_f^N B(\nu)d\nu = 1$, which gives $B_0 = (p - 1)f^{p-1}/(1 - \hat{f}^{p-1})$ for $p \neq 1$, where $\hat{f} = f/N$, and N is the Brunt–Väisälä frequency.

The model spectrum given by Eq. (17) does not distinguish between upward- and downward-propagating gravity waves—that is, between $m < 0$ and $m > 0$. Equation (5) indicates that the sign of the correlation between perturbations of the lapse rate and vertical velocity depends on the direction of phase propagation of each wave. Thus, we seek to represent the *net* spectrum.

If we denote the fractions of the total energy E_0 associated with waves with upward and downward phase velocities by E_+ and E_-, respectively, and assume that the spectral shapes of the two components are the same, then using the model in Eq. (17) to represent a spectrum of gravity wave amplitudes in Eq. (16), we obtain

$$\bar{w} = \Delta\alpha \int\int \frac{m}{\nu} \hat{w}^2(\mu, \nu)d\mu d\nu$$

$$= E_0\Delta\alpha \int_0^\infty mA(\mu)d\mu \int_f^N \frac{1}{\nu}\left(\frac{\nu}{N}\right)^2 B(\nu)d\nu, \quad (18)$$

where $\Delta\alpha = (E_+ - E_-)/E_0$ is a measure of the vertical anisotropy.

Integration of Eq. (18) leads to

$$\bar{w} = \frac{\sqrt{2}m_* E_0\Delta\alpha(p - 1)\hat{f}^{p-1}(1 - \hat{f}^{2-p})}{N(2 - p)(1 - \hat{f}^{p-1})}, \quad p \neq 1, 2,$$

or

$$\bar{w} = \sqrt{2}m_* E_0\Delta\alpha \frac{\hat{f}}{(1 - \hat{f})N} \ln(\hat{f}^{-1}), \quad p = 2. \quad (19)$$

The model used in Eq. (17) can also be used to express the wave energy E_0 in terms of the variance of the vertical velocity, σ_w^2:

$$\sigma_w^2 = \frac{\hat{w}^2}{2} = \frac{E_0}{2} \int_0^\infty A(\mu)d\mu \int_f^N \left(\frac{\nu}{N}\right)^2 B(\nu)d\nu$$

$$= \frac{E_0}{2}\frac{B_0}{N^2} \int_f^N \nu^{2-p}d\nu \quad (20)$$

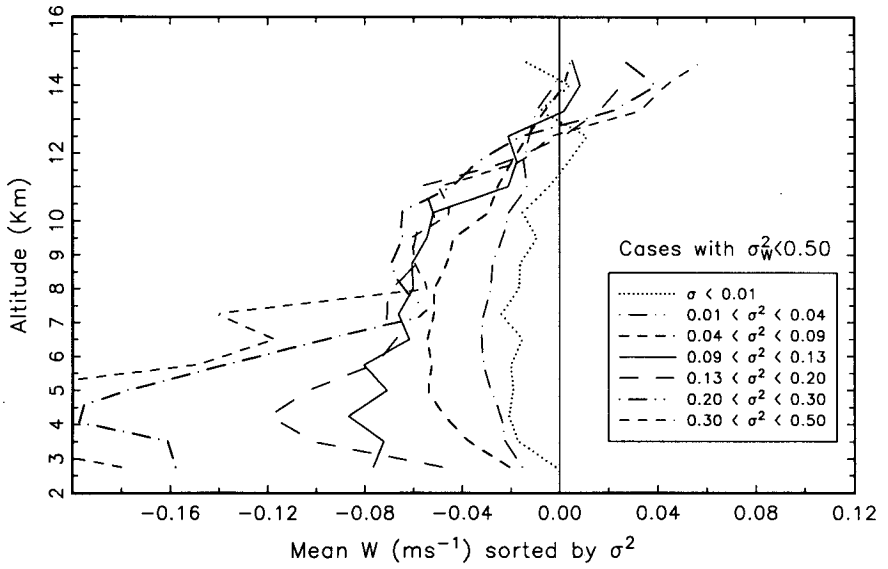

FIG. 7. Mean vertical velocities at Flatland during September 1990–August 1991 sorted according to hourly variance of the vertical velocity. Hours with $\sigma_w^2 > 0.5$ m^2 s^{-2} were not used.

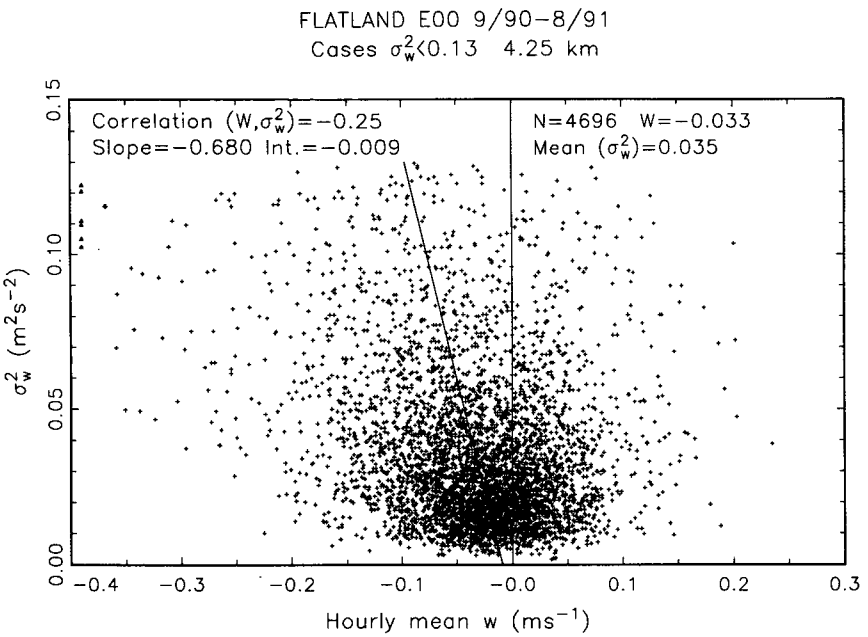

FIG. 8. Joint distribution of hourly $\bar{w}$ and σ_w^2 at Flatland at 4.25 km during September 1990–August 1991. The least-squares regression line is given. Hours with $\sigma_w^2 > 0.13$ m^2 s^{-2} were not used. The linear correlation coefficient is −0.25, the number of hours of data used is 4696, and the slope and intercept of the regression line is −0.68 and −0.009 m s^{-1}, respectively.

or

$$E_0 = 2\sigma_w^2 \frac{(3-p)(1-\hat{f}^{p-1})}{(p-1)(1-\hat{f}^{3-p})}\hat{f}^{1-p}, \quad p \neq 1, 2. \quad (21)$$

With $\hat{f} = 1/120$ and $p = 5/3$, then $E_0 = 93.5\sigma_w^2$. Measured values of σ_w^2 are about 0.1 m^2 s^{-2} throughout the troposphere at Flatland, although VanZandt et al. (1991) point out that observed values are slightly reduced relative to intrinsic values because of Doppler shifting. Then $E_0 \approx 10$ m^2 s^{-2}, which is within the range of recent estimates (e.g., Fritts and Lu 1993).

Expressing Eq. (19) in terms of σ_w^2 we have

$$\bar{w} = \begin{cases} \dfrac{4\pi\sqrt{2}\sigma_w^2\Delta\alpha}{\lambda_z^* N}\dfrac{(3-p)}{(2-p)}\dfrac{(1-\hat{f}^{2-p})}{(1-\hat{f}^{3-p})}, & p \neq 1, 2, \text{ or} \\ \dfrac{4\pi\sqrt{2}\sigma_w^2\Delta\alpha}{\lambda_z^* N(1-\hat{f})}\ln(\hat{f}^{-1}), & \text{for } p = 2. \end{cases} \quad (22)$$

With $\hat{f} = 1/120$, $N = 10^{-2}$ s^{-1}, and $p = 5/3$, then

$$\bar{w} = 5677\frac{\sigma_w^2\Delta\alpha}{\lambda_z^*}. \quad (23)$$

The coefficient in Eq. (23) varies with p; for example, it is 4848 and 8510 for $p = 3/2$ and 2, respectively. Recent estimates of λ_z^* are on the order of 2000–3000 m, with uncertainties of 50% or more (e.g., VanZandt et al. 1991). The uncertainty of $\Delta\alpha$ is also very large, but the value may be on the order of $-1/5$ (i.e., 3/5 with downward phase propagation and 2/5 with upward). These estimates of the variables in Eq. (23) give $\bar{w} \approx -5$ cm s^{-1} with an uncertainty of about a factor of 2. This value is very near the observed values of $\bar{w}$. Further, it is noteworthy that the use of a different form of the variables-separated spectrum in Eq. (17) would change only the coefficient in Eq. (23) and not the functional dependence. Finally, since observations clearly show that $A(\mu)$ is concentrated near m_* and $B(\nu)$ near f, the coefficient itself is relatively robust.

4. Correlation of mean vertical velocity with vertical velocity variance

Equations (16) and (23) predict a correlation between mean observed vertical velocity in radar observations $\bar{w}$ and the gravity wave amplitude for a monochromatic wave or the variance of vertical velocity σ_w^2 for a spectrum of waves. These predictions have been tested using observations from the Flatland radar. Since Flatland is located in the very flat terrain near Champaign–Urbana, Illinois, the data used should include few, if any, orographic effects. Figure 7 shows vertical profiles of $\bar{w}$ as a function of hourly σ_w^2 for the entire year September 1990–August 1991. Following quality control checking, the mean and variance of w were computed each hour at each level; the means were then sorted into bins depending on their associated variance, and the mean of each bin is plotted in Fig. 7. Clearly, as σ_w^2 increases the magnitude of $\bar{w}$ increases throughout the troposphere for small σ_w^2. Below about 7.5 km the largest values of σ_w^2, greater than about 0.13

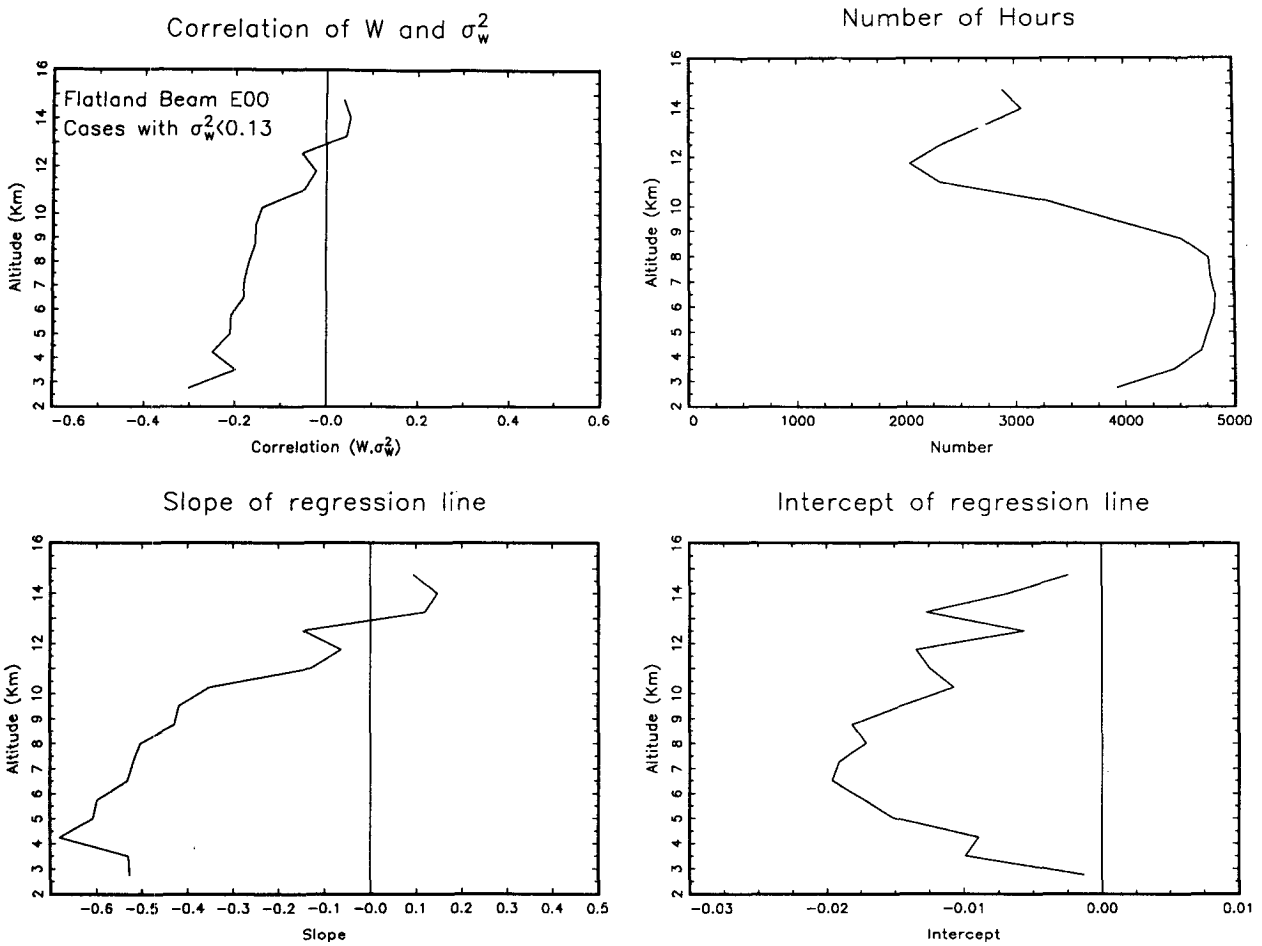

FIG. 9. Vertical profiles of the correlation, number of hours of data, slope, and intercept of the linear regression line of hourly values of $\bar{w}$ and σ_w^2 at Flatland during September 1990–August 1991.

$m^2\ s^{-2}$, apparently represent cases when falling precipitation contaminated the observations (e.g., Pauley et al. 1994). Above about 7.5 km, there is no apparent correlation between σ_w^2 and $\bar{w}$ when $\sigma_w^2 > 0.13\ m^2\ s^{-2}$, perhaps signaling a breakdown of the linear theory in cases of large amplitudes. Only cases with $\sigma_w^2 < 0.13\ m^2\ s^{-2}$ will be used further.

Figure 8 shows a scatterplot of σ_w^2 and $\bar{w}$ for data at 4.25 km. The correlation is −0.25 based on 4696 points, which is statistically significant above the 99% level. The linear regression line

$$\bar{w}_{\text{est.}} = A\sigma_w^2 + B \tag{24}$$

has $A = -0.68$ and $B = -0.009\ m\ s^{-1}$ at this altitude. Of course, we have implicitly assumed that the relationship between σ_w^2 and $\bar{w}$ implied in Eq. (16) applies in every case. This assumption does not hold in many cases where the gravity waves are not propagating vertically but are trapped (i.e., $m = 0$), yet $\bar{w}$ is nonzero owing to other causes such as synoptic-scale motion systems. The point is that some of the scatter seen in Fig. 8 is likely due to trapped waves.

The correlation coefficient, number of hourly data available, and slope and intercept of the regression line (A and B) as functions of altitude for all data during the year are shown in Fig. 9. The number of hours of data falls off rapidly above about 10 km and then shows a small secondary peak in the lower stratosphere owing to specular reflections. The slope of the regression line is only slowly varying throughout the midtroposphere, varying between about −0.4 and −0.6. The intercept ranges from about −0.01 to −0.02 $m\ s^{-1}$ at these heights.

Figure 10 illustrates the relationship between σ_w^2 and $\bar{w}$ for bimonthly periods in 1990–91. These results show that the relationship between σ_w^2 and $\bar{w}$ changes little during the year. Values of the slope and intercept from linear correlation for all data in the layer 3.5 to 9.5 km are given in each panel for each bimonthly period.

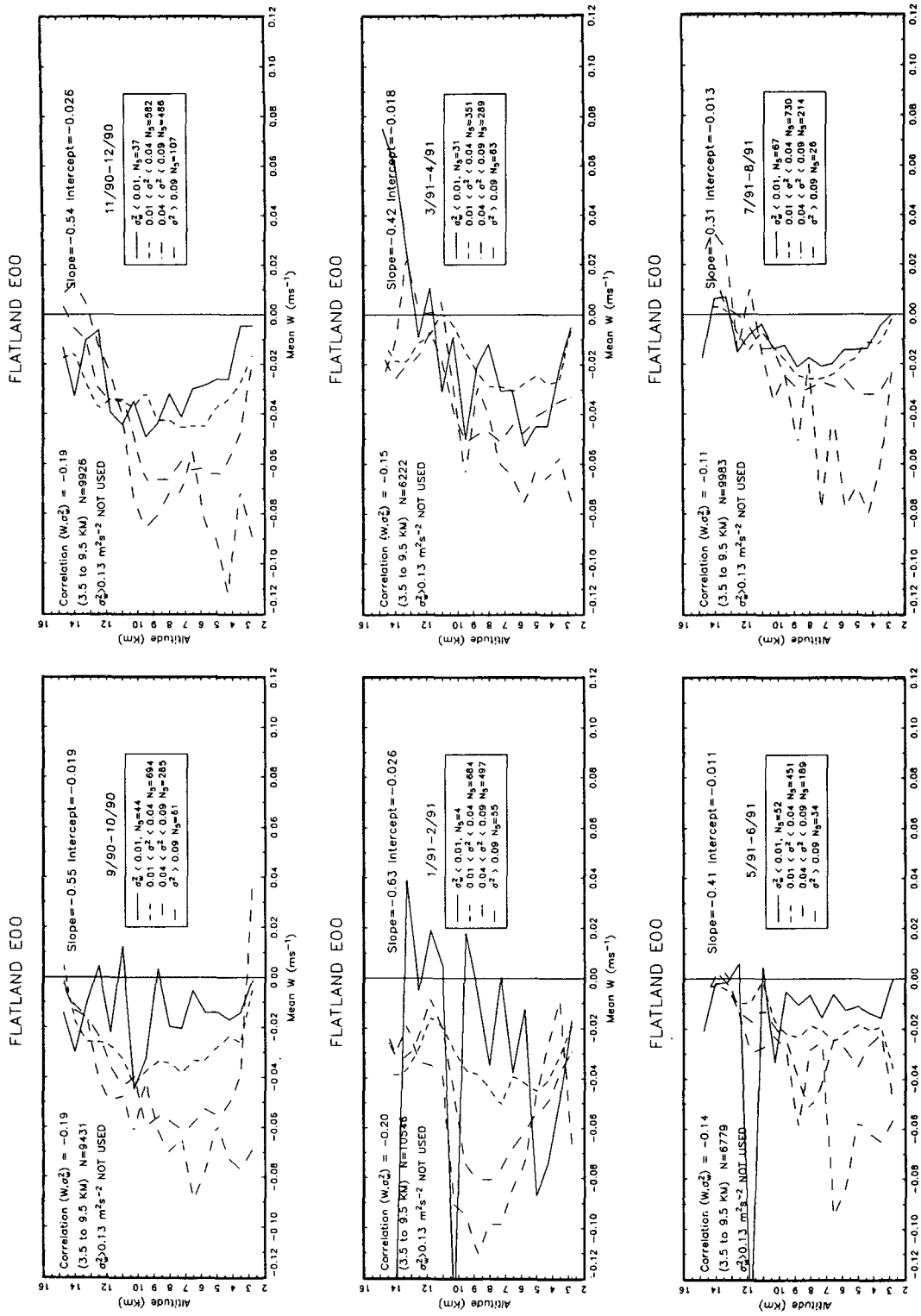

FIG. 10. Mean vertical velocities for bimonthly periods at Flatland during September 1990–August 1991 sorted according to hourly variance of the vertical velocity. Hours with $\sigma_w^2 > 0.13$ m^2 s^{-2} were not used. The correlation coefficient, number of hours of data used, and slope and intercept of the regression line for all data in the height range 3.5–9.5 km are fairly uniform throughout the year.

Values of the slope A range from -0.31 to -0.63, and the mean value is about -0.55.

5. Discussion

The average value of the slope A of the regression line in the troposphere below 10 km is -0.55. Equating the coefficients of σ_w^2 in Eqs. (23) and (24) yields

$$\Delta\alpha = \frac{A\lambda_z^*}{5677}. \tag{25}$$

Taking $A = -0.55$ and $\lambda_z^* \approx 2.0$ km gives $\Delta\alpha \approx -0.2$. It is noteworthy that this estimate of $\Delta\alpha$ is consistent with a dominant source of gravity waves at Flatland in the boundary layer, as expected. Also, it is gratifying that since $|\Delta\alpha|$ must be less than or equal to 1, then λ_z^* must be at most 10 km, which is larger than any reasonable value of λ_z^* that has been inferred from observations.

The intercept B is the value of $\bar{w}$ due to nonrandom factors besides reflectivity changes in gravity waves, such as mean motions associated with the general circulation or with quasi-permanent circulation features such as stationary troughs. The mean value of B below 10 km is about -0.015 m s^{-1}. As noted earlier, the vertical component of quasi-horizontal flow on isentropic surfaces during winter 1990 was -0.014 m s^{-1}.

6. Summary and conclusions

The mean vertical motions observed using the VHF radar at Flatland, Illinois, and Liberal, Kansas, are downward in the troposphere, ranging in magnitude from about 3 to 7 cm s^{-1}. They go to zero near the tropopause and are often slightly positive in the lower stratosphere. These mean values are observed to be downward regardless of whether the sky is clear or cloudy, regardless of time of day, and regardless of season. During the winter season analyzed in this study the flow along sloping isentropic surfaces appears to account for about a centimeter per second of downward motion.

It is suggested that the dominant effect causing observations of $\bar{w} \neq 0$ is small changes in the refractive index induced by vertically propagating gravity waves. In waves with downward phase propagation, the vertical velocity and static stability are negatively correlated; thus, regions of downward-moving air have higher reflectivity on a statistical basis in such waves. The model for $\bar{w}$ developed here applies to reflections from isotropic and anisotropic turbulent eddies as well as Fresnel scattering. The measured $\bar{w}$ are thus largely "apparent" mean vertical motion.

Downward phase propagation is associated with upward energy propagation in gravity waves. Our results are thus consistent with a lower-tropospheric source of gravity waves, perhaps due to instabilities in the planetary boundary layer as discussed by Nastrom et al. (1990a), among others. If the waves launched in the lower troposphere are selectively filtered in the upper troposphere, such as at critical levels on the boundary of the jet stream near the tropopause, then $\Delta\alpha$ could become very small in the upper troposphere and could account for the tendency for $\bar{w}$ to approach zero at the tropopause. Resolution of this issue is beyond the scope of our present study.

The linear gravity wave model predicted a correlation between σ_w^2 and $\bar{w}$. Observations at Flatland verify that this correlation exists throughout the troposphere and during all seasons. Linear regression of $\bar{w}$ with σ_w^2 with the Flatland data produced coefficients that can be used to estimate values of gravity wave field parameters such as $\Delta\alpha$. Our estimate that 60% of the waves have downward phase propagation in the troposphere is within limits that are consistent with past estimates of other gravity wave field parameters such as λ_z^*.

This study has focused on measured mean vertical motions and the effects of gravity waves. While the discussion has emphasized effects seen with Doppler radars in the troposphere, the model for $\bar{w}$ presented here applies to the reflectivity from any refractive-index irregularities that can be treated as passive scalars, whether they are in neutral atmospheric density, aerosol density, or plasma density and whether they arise from isotropic turbulence, anisotropic turbulence, Fresnel scattering, etc. No effort has been made here to estimate the possible influence of gravity waves on other variables measured by wind profilers, such as the vertical flux of horizontal momentum.

Acknowledgments. This study was partially supported by NSF Grants ATM-9005979 and ATM-8816104. We are grateful for comments from W. L. Clark, M. Crochet, and J. M. Warnock.

REFERENCES

Balsley, B. B., W. L. Ecklund, D. A. Carter, A. C. Riddle, and K. S. Gage, 1988: Average vertical motions in the tropical atmosphere observed by a radar wind profiler on Pohnpei (7° latitude, 157° longitude). *J. Atmos. Sci.*, **45**, 396–405.

Clark, W. L., S. Henson, P. Johnston, G. D. Nastrom, T. E. VanZandt, and J. M. Warnock, 1993: Flatland wind profiler system verification and calibration for measurement of large-scale vertical motion. Preprints, *Eighth Symp. on Meteorological Observations and Instrumentation,* Anaheim, Amer. Meteor. Soc., 186–188.

Crochet, M., F. Cuq, F. M. Ralph, and S. V. Venkateswaran, 1990: Clear-air radar observations of the great October storm of 1987. *Dyn. Atmos. Ocean.*, **14**, 443–461.

Desaubies, Y. J. F., 1976: Analytical representation of internal wave spectra. *J. Phys. Oceanogr.*, **6**, 976–981.

Ecklund, W. L., K. S. Gage, B. B. Balsley, R. G. Strauch, and J. L. Green, 1982: Vertical wind variability observed by VHF radar in the lee of the Colorado Rockies. *Mon. Wea. Rev.*, **110**, 1451–1457.

Fritts, D. C., 1984: Gravity wave saturation in the middle atmosphere: A review of theory and observations. *Rev. Geophys. Space Phys.*, **22**, 275–308.

——, and W. Lu, 1993: Spectral estimates of gravity wave energy and momentum fluxes. II: Parameterization of wave forcing and variability. *J. Atmos. Sci.*, **50**, 3695–3713.

Fukao, S., M. F. Larsen, M. D. Yamanaka, H. Furukawa, T. Tsuda, and S. Kato, 1991: Observations of a reversal in long-term average vertical velocities near the jet stream wind maximum. *Mon. Wea. Rev.*, **119,** 1479–1489.

Gage, K. S., 1990: Radar observations of the free atmosphere: Structure and dynamics. *Radar in Meteorology,* David Atlas, Ed., Amer. Meteor. Soc., 535–564.

——, J. R. McAfee, D. A. Carter, W. L. Ecklund, A. C. Riddle, G. C. Reid, and B. B. Balsley, 1991: Long-term mean vertical motion over the tropical Pacific: Wind-profiling Doppler radar measurements. *Science,* **254,** 1771–1773.

Green, J. L., W. L. Clark, J. M. Warnock, and G. D. Nastrom, 1986: A comparison of vertical velocities measured from specular and nonspecular echoes by a VHF radar. *Handbook for MAP,* **20,** 263–272. [Available from SCOSTEP Secretariat, University of Illinois, 1406 W. Green St., Urbana, IL 61801.]

——, K. S. Gage, T. E. VanZandt, W. L. Clark, J. M. Warnock, and G. D. Nastrom, 1988: Observations of vertical velocity over Illinois by the Flatland radar. *Geophys. Res. Lett.*, **15,** 269–272.

Holton, J. R., 1979: *An Introduction to Dynamic Meteorology.* Academic Press, 391 pp.

Kudeki, E., P. K. Rastogi, and F. Surucu, 1993: Systematic errors in radar wind estimation: Implications for comparative measurements. *Radio Sci.,* **28,** 169–180.

McAfee, J. R., K. S. Gage, and R. G. Strauch, 1993: A comparison of vertical velocities measured by the 50 MHz and 404 MHz profilers at Platteville, Colorado. Preprints, *26th Conf. on Radar Meteorology,* Norman, Amer. Meteor. Soc., 561–563.

Nastrom, G. D., and K. S. Gage, 1984: A brief climatology of vertical wind variability in the troposphere and stratosphere as seen by the Poker Flat, Alaska, MST radar. *J. Climate Appl. Meteor.,* **23,** 453–460.

——, W. L. Ecklund, and K. S. Gage, 1985: Direct measurement of large-scale vertical velocities using clear-air Doppler radars. *Mon. Wea. Rev.,* **113,** 708–718.

——, M. R. Peterson, J. L. Green, K. S. Gage, and T. E. VanZandt, 1990a: Sources of gravity wave activity seen in the vertical velocities observed by the Flatland VHF radar. *J. Appl. Meteor.,* **29,** 783–792.

——, T. E. VanZandt, W. L. Clark, J. M. Warnock, J. L. Green, and K. S. Gage, 1990b: Diagnosis of a downward bias in the vertical motions seen by VHF clear-air Doppler radars. *Eos,* **71,** 28 (abstract only).

——, W. L. Clark, K. S. Gage, T. E. VanZandt, and J. M. Warnock, 1993: Studies of the mean vertical motions seen by VHF wind profilers in Illinois and Kansas. Preprints, *Eighth Symp. on Meteorological Observations and Instrumentation,* Anaheim, Amer. Meteor. Soc., 200–204.

Palmer, R. D., M. F. Larsen, R. F. Woodman, S. Fukao, M. Yamamoto, T. Tsuda, and S. Kato, 1991: VHF radar interferometry measurements of vertical velocity and the effect of tilted refractivity surfaces on standard Doppler measurements. *Radio Sci.,* **26,** 417–428.

Pauley, P. M., R. L. Creasey, W. L. Clark, and G. D. Nastrom, 1994: Comparisons of horizontal winds measured by opposing beams with the Flatland ST radar and between Flatland measurements and NMC analyses. *J. Atmos. Oceanic Technol.,* **11,** 256–274.

Tsuda, T., P. T. May, T. Sato, S. Kato, and S. Fukao, 1988: Simultaneous observations of reflection echoes and refractive index gradient in the troposphere and lower stratosphere. *Radio Sci.,* **23,** 655–665.

Van den Dool, H. M., 1990: Time-mean precipitation and vertical motion patterns over the United States. *Tellus,* **42A,** 51–64.

VanZandt, T. E., and D. C. Fritts, 1989: A theory of enhanced saturation of the gravity wave spectrum due to increases in atmospheric stability. *Pure Appl. Geophys.,* **130,** 399–420.

——, G. D. Nastrom, and J. L. Green, 1991: Frequency spectra of vertical velocity from Flatland VHF radar data. *J. Geophys. Res.,* **96,** 2845–2855.

Warnock, J. M., W. L. Clark, T. E. VanZandt, K. S. Gage, G. D. Nastrom, P. E. Johnston, and S. W. Henson, 1993: Enhancements to the Flatland Atmospheric Observatory. Preprints, *Eighth Symp. on Meteorological Observations and Instrumentation,* Anaheim, Amer. Meteor. Soc., 225–230.

Weber, B. L., D. B. Wuertz, D. C. Law, A. S. Frisch, and J. M. Brown, 1992: Effects of small-scale vertical motion on radar measurements of wind and temperature profiles. *J. Atmos. Oceanic Technol.,* **9,** 193–209.